Structural, Spectroscopic, Magnetic and Thermal Properties in the $[SrM(C_3H_2O_4)_2(H_2O)_5] \cdot 2\ H_2O$ (M = Mn, Fe, Co, Ni) System: Precursors of $SrMO_{3-x}$ Mixed Oxides

Izaskun Gil de Muro,[a] Maite Insausti,[a] Luis Lezama,[a] José L. Pizarro,[b] Maria I. Arriortua,[b] and Teófilo Rojo*[a]

Keywords: Malonate / Mixed oxides / Crystal structure / Thermochemistry / Magnetic properties

The $[SrM(C_3H_2O_4)_2(H_2O)_7]$ (M = Mn, Fe, Co, Ni) compounds have been prepared and characterised by chemical analysis and X-ray diffraction. The crystal structure of $[SrCo(C_3H_2O_4)_2(H_2O)_5] \cdot 2\ H_2O$ has been solved [monoclinic, $P2_1/c$, $Z = 4$, $a = 6.880(1)$, $b = 14.360(2)$, $c = 15.800(2)$ Å. $\beta = 101.69(1)°$]. The compound exhibits a three-dimensional chain/snake structure consisting of $-CoO_6-[SrO_7]_\infty-CoO_6-$ repeating units parallel to the [0 1 1] and [0 –1 1] directions. UV/Vis data are consistent with the cations being in a high-spin octahedral symmetry. Magnetic measurements show antiferromagnetic interactions for all compounds with approximate θ values of –0.5 K, except for the cobalt compound (–24.5 K) where the decrease of the $\chi_m T$ curve can also be attributed to the spin-orbit coupling. Thermal analyses performed in air and under nitrogen show three consecutive steps: dehydration, ligand pyrolysis, and inorganic residue evolution. Thermal treatments in tubular furnaces were performed in order to obtain pure $SrMO_{3-x}$ phases. In all cases the oxides are nonstoichiometric and oxygen-deficient with structures related to that of perovskite. Lower temperatures and reaction times than those given in the literature have been used when using the ceramic method. These "soft" treatments gave rise to homogeneous particles of small grain size.

Introduction

Since the discovery of high-temperature superconducting oxides, much interest has been paid to the 3d transition metal oxides. In particular, the electronic states of the perovskite-type oxides have been extensively investigated from the standpoint of 3d band filling,[1−3] those that have transition metal ions such as Mn^{4+}, Fe^{4+}, Co^{4+}, Ni^{3+}, or Cu^{3+} in unusually high oxidation states, as well as mixed valence states, being those most studied.

The physical properties of these kinds of oxides depend greatly upon the oxidation state and the location of the cation at either tetrahedral or octahedral sites. The electronic and magnetic properties of the $SrFeO_{3-x}$ system vary a great deal with the oxidation state of the iron ions, ranging from the antiferromagnetic insulator oxide $SrFeO_{2.5}$, a brown millerite-type structure, to the antiferromagnetic metallic compound $SrFeO_3$, with cubic perovskite structure.[4] The $SrMnO_{3-x}$ phase becomes increasingly anion-deficient in air with increasing temperature.[5] For this reason the physical properties related to the crystal structures have been studied.[6] In the case of the cobalt oxides, the named cobaltites have attracted special attention due to their application as low-cost fuel-cell electrodes.[7]

In addition to the oxidation state, the physical properties also depend on either the final particle size or the preparative methods used to obtain the materials. In the last few years, "soft" chemical routes have often been employed to prepare advanced ceramic powders, as an alternative method to the conventional ceramic method. The solid solution precursor technique used for the preparation of fine oxide materials at low temperatures in this way has frequently been reported.[8] This method is quite advantageous, due to the excellent stoichiometry and low impurity content of the final phases.[9]

We are interested in the study of organometallic compounds with carboxylates, as well as their use as precursor materials for obtaining mixed oxides.[10] The chemistry of transition metal complexes involving malonate as a bridging ligand has been investigated due to a wide variety of physical properties,[11] the results concerning magnetic properties of 1D, 2D, and 3D systems being of special interest.[12]

Recently, a series of metal malonate complexes has been reported.[13] In this paper, the synthesis and characterisation of the $[SrM(C_3H_2O_4)_2(H_2O)_7]$ (M = Mn, Fe, Co, Ni) compounds is presented. Hereafter, these complexes will be denoted as SrMn, SrFe, SrCo, and SrNi, respectively. Spectroscopic and magnetic studies have been performed on these compounds. In order to obtain information concerning the formation of pure mixed oxides from the organometallic precursors, a detailed thermal study has been carried out.

[a] Departamento de Química Inorgánica, Facultad de Ciencias. Universidad del País Vasco,
Apdo. 644, E-48080 Bilbao, Spain
[b] Departamento de Mineralogía-Petrología, Facultad de Ciencias. Universidad del País Vasco,
Apdo. 644, E-48080 Bilbao, Spain
Fax: (internat.) + 34-94/464-8500
E-mail: qiproapt@lg.ehu.es

  1434−1948/99/0606−0935 $ 17.50+.50/0

Results and Discussion

The synthesis of the complexes was performed as described in the Experimental Section. Crystal structure analyses were performed for the $[SrCo(C_3H_2O_4)_2(H_2O)_7]$ complex. Crystal data and details of the structure determination are summarized in Table 1. Bond lengths and angles for non-hydrogen atoms are given in Table 2.

Table 1. Data collection and structure refinement for the $[SrCo(C_3H_2O_4)_2(H_2O)_5] \cdot 2\ H_2O$ compound

Molecular Formula	$C_6H_{18}CoO_{15}Sr$
a [Å]	6.880(1)
b [Å]	14.360(2)
c [Å]	15.800(2)
β	101.69(1)°
V [Å^3]	1528.6(4)
Z	4
Molecular mass [g]	476.75
Space group	$P2_1/c$
T [°C]	293(2)
$\rho_{obsd.}$ [g cm^{-3}]	2.07(6)
$\rho_{calcd.}$ [g cm^{-3}]	2.054
μ [mm^{-1}]	4.651
λ [Å]	0.71070
$R(F_o)$[a]	0.0427
$R_w(F_o^2)$[b]	0.0967

[a] $R_1(F_o) = [\Sigma||F_o| - |F_c||/\Sigma|F_o|]$. — [b] $wR_2(F_o^2) = \{\Sigma[w(F_o^2 - F_c^2)^2]/\Sigma[w(F_o^2)^2]\}^{1/2}$

The asymmetric unit consists of diaquobis(malonato)cobaltate(II) anions linked to strontium ions and two water molecules of crystallization, O(6w) and O(7w) (see Figure 1). The cobalt(II) centres adopt an octahedral coordination pattern. The polyhedron is formed by the four carboxylate groups from the two malonate ions and the O(1w) and O(2w) water molecules, which are located in the axial plane. The O(1), O(5), O(3), and O(7) atoms are coplanar at average distances of 2.06 Å. The O−Co−O angles are close to 90°, in good agreement with those observed for other related compounds.[13][14] The cobalt atom is raised by 0.016(1) Å above the square plane in the direction of O(2w). The distortion around the cobalt(II) ion has been calculated by quantification of the Muetterties and Guggenberger description.[15] The value obtained, $\Delta = 0.04$, is indicative of a quite regular octahedron.

The strontium ions are surrounded by nine oxygen atoms, five of them belonging to three malonate groups, and four water molecules, O(3w), O(3w)^3, O(4w), O(5w), forming an irregular polyhedron. The average Sr−O distance is 2.67 Å. The strontium polyhedra are linked between them along the [1 0 0] direction via two different common edges, O(8)^1−O(8)^2 and O(3w)−O(3w)^3, due to the presence of an inversion centre at the middle point of these edges [at x = 0 and 1/2, for O(8)^1−O(8)^2 and O(3w)−O(3w)^3, respectively]. The Sr−O(8)−Sr and Sr−O(3w)−Sr angles are both 113.9(2)°. These $[SrO_7]_\infty$ chains, running along the [100] direction, are linked between them by corner-sharing CoO_6 distorted octahedra, where O(1) and O(7) oxygens are the common corners. These connections form new "perpendicular" chains parallel to [0 1 1] and [0 −1 1] directions

Table 2. Selected bond lengths [Å] and angles [°] for the $[SrCo(C_3H_2O_4)_2(H_2O)_5] \cdot 2\ H_2O$ compound; symmetry transformations used to generate equivalent atoms: (1): $-x + 1$, $y - 1/2$, $-z + 1/2$; (2): x, $-y + 1/2$, $z + 1/2$; (3): $-x$, $-y$, $-z + 1$; (4): $-x + 1$, $-y$, $-z + 1$; (5): x, $-y + 1/2$, $z - 1/2$; (6): $-x + 1$, $y + 1/2$, $-z + 1/2$

Sr−O(8)^1	2.583(4)	O(2)−C(1)	1.249(7)
Sr−O(2)	2.595(4)	O(3)−C(3)	1.261(7)
Sr−O(4w)	2.596(4)	O(4)−C(3)	1.238(7)
Sr−O(5w)	2.599(4)	O(5)−C(4)	1.259(7)
Sr−O(3w)	2.665(4)	O(6)−C(4)	1.243(7)
Sr−O(8)^2	2.675(4)	O(7)−C(6)	1.252(7)
Sr−O(7)^2	2.737(4)	O(8)−C(6)	1.246(7)
Sr−O(3w)^3	2.752(4)	O(8)−Sr^6	2.583(4)
Sr−O(1)	2.847(4)	O(8)−Sr^5	2.675(4)
Co−O(3)	2.047(5)	C(1)−C(2)	1.504(9)
Co−O(5)	2.050(4)	C(2)−C(3)	1.493(9)
Co−O(1)	2.068(4)	C(2)−H(21)	0.97
Co−O(7)	2.091(4)	C(2)−H(22)	0.97
Co−O(1w)	2.096(5)	C(4)−C(5)	1.514(8)
Co−O(2w)	2.128(4)	C(5)−C(6)	1.519(8)
O(1)−C(1)	1.250(7)	C(5)−H(51)	0.97
		C(5)−H(52)	0.97
O(8)1−Sr−	91.42(14)	O(2)−Sr−O(8)^2	148.71(14)
O(2)−Sr−O(4w)	93.44(14)	O(2)−Sr−O(1)	47.05(12)
O(2)−Sr−O(5w)	119.17(13)	O(4w)−Sr−O(1)	67.85(13)
O(2)−Sr−O(3w)	76.86(13)	O(4w)−Sr−O(3w)	136.36(14)
O(3)−Co−O(5)	178.7(2)	O(3)−Co−O(1)	88.9(2)
O(5)−Co−O(1)	91.9(2)	O(3)−Co−O(2w)	88.9(2)
O(1)−Co−O(1w)	91.4(2)	O(1)−Co−O(7)	179.1(2)
O(1)−Co−O(2w)	92.9(2)	O(1w)−Co−O(2w)	175.0(2)
Sr−O(3 W)−Sr^3	113.9(2)	C(1)−O(1)−Co	127.9(4)
C(6)−O(7)−Co	126.0(3)	C(1)−O(1)−Sr	88.7(3)
C(6)−O(7)−Sr^5	93.2(3)	Co−O(1)−Sr	143.4(2)
Co−O(7)−Sr^5	140.6(2)	C(1)−O(2)−Sr	100.7(4)
C(6)−O(8)−Sr^6	149.2(4)	C(3)−O(3)−Co	130.4(4)
C(6)−O(8)−Sr^5	96.3(3)	C(4)−O(5)−Co	127.5(4)
Sr^6−O(8)−Sr^5	113.87(14)	O(4)−C(3)−O(3)	123.4(6)
O(2)−C(1)−O(1)	121.9(5)	O(4)−C(3)−O(3)	123.4(6)
C(3)−C(2)−C(1)	125.2(6)	O(6)−C(4)−O(5)	122.5(6)
O(8)−C(6)−O(7)	122.7(5)	C(4)−C(5)−C(6)	118.6(5)
H(21)−C(2)−H(22)	106.3	H(51)−C(5)−H(52)	107.1

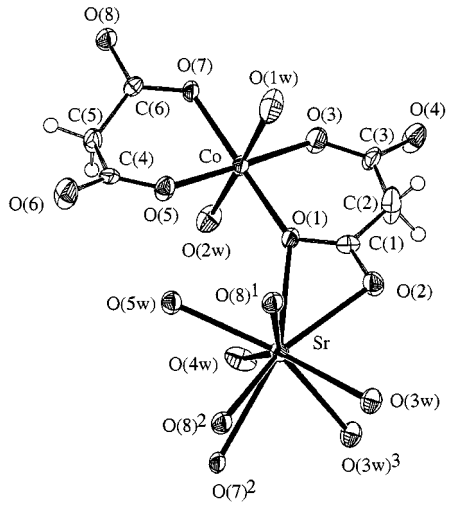

Figure 1. View of the coordination polyhedra for strontium and cobalt ions with atom numbering for the $[SrCo(C_3H_2O_4)_2(H_2O)_5] \cdot 2\ H_2O$ compound

formed by $-CoO_6-[SrO_7]_\infty-CoO_6-$ units, as can be seen in Figure 2. In these chains, the Co···Co^2 direct distance is 7.908(2) Å and the exchange distance through the O(1)−Sr−O(7)^2 atoms is 9.74 Å. In this way, the structure

could be described as a three dimensional package of strontium dimers linked through CoO_6 polyhedra. (1: $1 - x$, $y - 1/2$, $1/2 - z$; 2: x, $1/2 - y$, $1/2 + z$; 3: $-x$, $-y$, $1 - z$).

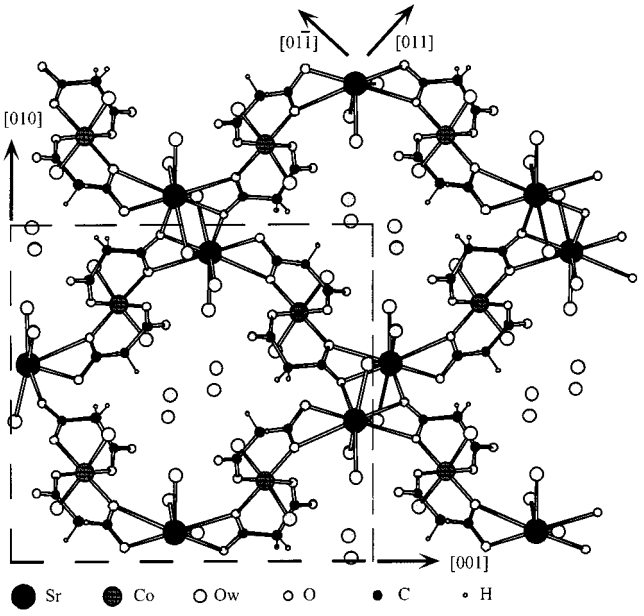

Figure 2. A perspective view of the $[SrCo(C_3H_2O_4)_2(H_2O)_5] \cdot 2\,H_2O$ compound in the *bc* plane

In the malonate ligands, the dihedral angle between the planes O(5)−C(4)−O(6) and O(7)−C(6)−O(8) is 143.8(7)° and between O(4)−C(3)−O(3) and O(1)−C(1)−O(2) it is 9.4(5)°. The chelated malonate ring formed by the O(5)−C(4)−C(5)−C(6)−O(7) atoms has an envelope conformation in which only the methylene group is significantly displaced from the ring plane, while the other ring formed by the O(3)−C(3)−C(2)−C(1)−O(1) atoms is quite planar. The difference in the C(3)−C(2)−C(1), 125.2(6)° and C(4)−C(5)−C(6), 118.6(5)° angles could be explained on the basis of these linkages and the conformation of the ligands. In both malonate ions, the average C−O distances and O−C−O angles are 1.25 Å and 122.6°, respectively. All the oxygen atoms belonging to the malonate ligand are bonded to one or two metal ions, except the O(4) and O(6) atoms which are uncoordinated.

In the crystal structure, extensive hydrogen bonds involving the carboxyl groups and water molecules could be described by acceptor-donor distances of ca. 3 Å. However, the difficulty in locating the water hydrogen atoms prevents us from predicting this kind of bonding in the structure.

For the SrMn, SrFe, and SrNi phases, high-quality crystals were not obtained. X-ray diffraction patterns of the microcrystalline products were performed in the 2θ range of 5−70°. Indexation of the diffraction profile and refinement of the cell parameters were made by FULLPROF (pattern-matching analysis)[16] on the basis of the space group, $P2_1/c$, and the cell parameters found for the SrCo phase. The calculated values are given in Table 3. Taking into account these results, the four phases can be considered to be isostructural.

Table 3. Crystallographic data for the $[SrM(C_3H_2O_4)_2(H_2O)_5] \cdot 2\,H_2O$ (M = Mn, Fe, Ni, Co) compounds

Compound	SrMn	SrFe	SrNi	SrCo
a [Å]	6.9517(3)	6.9105(3)	6.8762(5)	6.880(1)
b [Å]	14.5678(7)	14.4758(7)	14.296(1)	14.360(2)
c [Å]	15.7760(6)	15.7808(8)	15.889(1)	15.800(2)
β [°]	102.31(2)	102.03(3)	101.36(4)	101.69(1)
V [Å^3]	1560.9	1543.9	1531.3	1528.6(4)
Space group	$P2_1/c$	$P2_1/c$	$P2_1/c$	$P2_1/c$
Z	4	4	4	4

The IR spectra of the compounds show a strong broad absorption band in the region 3100−3600 cm^{-1}, corresponding to the stretching vibration of the hydroxy groups, ν(O−H), of the water molecules. The presence of a band at around 1580 cm^{-1} is attributed to the stretching vibration of the carbonyl group linked to the metal ions. This band appears together with the antisymmetric $\upsilon_a(COO^-)$ vibration. The bands corresponding to the symmetric $\upsilon_s(COO^-)$ vibration are localised in the 1380−1452 cm^{-1} range. The relative positions of these two bands, $\Delta = \upsilon_a(COO^-) - \upsilon_s(COO^-)$, are lower than those corresponding to the free malonic acid. This fact indicates that the coordination of the ligands to the metal ions could be through the formation of a chelate, giving rise to an electronic delocalization in the carboxylate group.[17] The presence of a shoulder at around 1700 cm^{-1} in the IR spectra could be attributed to the existence of C=O groups, which are not linked to any metal ions as was observed in the crystal structure of the SrCo compound. Nevertheless, the appearance of a broad band in this region, probably due to the presence of hydrogen bonds between the water molecules and the carboxylate groups, hampers the localization of free carboxylate groups in the IR spectra. Finally, the band observed for all compounds in the 1100−1300 cm^{-1} range corresponds to the bending vibration of the carbonyl group, δ(C=O).

Reflectance spectra were recorded for the $[SrM(C_3H_2O_4)_2(H_2O)_7]$ (M = Fe, Co, Ni) compounds. For the nickel phase the bands that appear at frequencies $\tilde{\nu}_1$ = 8930, $\tilde{\nu}_2$ = 13513 and $\tilde{\nu}_3$ = 26315 cm^{-1} have been assigned to the three allowed transitions $^3A_{2g} \rightarrow {}^3T_{2g}$, $^3T_{1g}$ (F) and $^3T_{1g}$(P). The spin-forbidden transitions $^3A_{2g} \rightarrow {}^1E_g$ and $^1T_{2g}$ were also observed $\tilde{\nu}_4$ = 15570 and $\tilde{\nu}_5$ = 21500 cm^{-1}, respectively. The Dq and Racah parameters, calculated by fitting the experimental frequencies to an energy level diagram for octahedral d^8 systems are: Dq = 893 cm^{-1}, B = 957 cm^{-1} and C = 4264 cm^{-1}, values usually found for octahedrally coordinated Ni^{II} compounds.[18] In the case of the $[SrCo(C_3H_2O_4)_2(H_2O)_7]$ compound, the positions of the bands are in the range usually found for Co^{II} ions in octahedral geometries, $\tilde{\nu}_1$ = 8550, $\tilde{\nu}_2$ = 16670 and $\tilde{\nu}_3$ = 20200 cm^{-1} which have been assigned to the $^4T_{1g} \rightarrow {}^4T_{2g}(F)$, $^4A_{2g}$ (F) and $^4T_{1g}(P)$ transitions. The Dq = 966 cm^{-1} and B = 851 cm^{-1} values confirm the octahedral geometry. For the

iron compound the band corresponding to the $^5T_{2g} \rightarrow {}^5E_g$ transition is split into two, due to the Jahn−Teller distortion of the ^5E_g energy level. From the position of these bands, 11235 and 6875 cm^{-1}, a value of $(8/3)d\sigma = 4360$ cm^{-1} was calculated. This fact is indicative of the presence of a slight distortion around the metal ion in this compound.

The X-band EPR spectra of polycrystalline samples of the $[SrM(C_3H_2O_4)_2(H_2O)_7]$ (M = Mn, Co) compounds have been performed in the temperature range 4.2−300 K. The spectra at 4 K are shown in Figure 3. In the case of the manganese phase broad and isotropic signals appear at room temp., and these signals are narrower at low temperatures. The corresponding g_{iso} parameter at 4 K has a value of 2.00, in good accordance with that corresponding to the Mn^{II} ions in octahedral geometry. The spectrum of the cobalt phase shows the strong anisotropy of the g factor. The signal presents a very broad linewidth due to the spin-orbit coupling which hampers the determination of good g values for this compound.

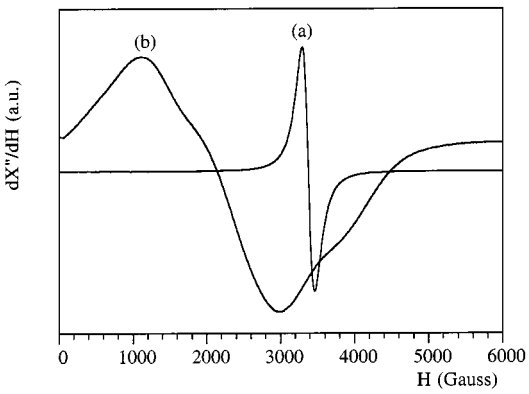

Figure 3. Powdered X-band ESR spectra for the $[SrM(C_3H_2O_4)_2(H_2O)_5] \cdot 2\,H_2O$ compounds at 4 K (a) M = Mn, (b) M = Co

Susceptibility magnetic measurements of the $[SrM(C_3H_2O_4)_2(H_2O)_7]$ (M = Mn, Co, Fe, Ni) compounds were carried out in the temperature range of 1.8−300 K. A similar magnetic behaviour was observed for the SrFe, SrNi, and SrMn phases. The $\chi_m{}^{-1}$ and $\chi_m T$ vs T curves for the Mn^{II} compound is represented in Figure 4a. The $\chi_m{}^{-1}$ vs T curves for these compounds show a Curie−Weiss behaviour in the range 5−300 K with negative intercepts of −0.68 K (SrFe), −0.36 K (SrNi), and −1.8 K (SrMn). These negative θ values and the overall appearance of the $\chi_m T$ vs T curves are indicative of the presence of antiferromagnetic interactions. The values for the Curie constants are 3.65, 1.18, and 4.36 cm^3 K/mol, respectively. The $\chi_m T$ products are practically temperature-independent for $T >$ 50 K, reaching values of 2.45 (SrFe), 1.12 (SrNi), 3.7 (SrMn) cm^3 K/mol when cooling from this temperature to 4.2 K. Taking into account the crystallographic description, the magnetic behaviour could be described on the basis of either a Heisenberg square-planar system or a 3D network. Nevertheless, in all cases the best least-squares fit leads to J/k values less than 1 K.

For the SrCo compound the high-temperature data ($T >$ 60 K) were also fitted to a Curie−Weiss law with θ = −24.5 K and $Cm = 3.77$ cm^3 $Kmol^{-1}$ of metal ion (Figure 4b). The continuous decrease in the $\chi_m T$ curve must be ascribed to the antiferromagnetic exchange interactions, together with the effect of the spin-orbit coupling ($\lambda = -170$ cm^{-1} for the free Co^{2+} ion),[19] which leads to an effective spin $S = 1/2$ for the system at low temperatures ($T <$ 30 K). This effect is qualitatively similar to those of the antiferromagnetic interactions, making difficult to distinguish between the contributions of these two effects on the whole magnetic behaviour of this compound.

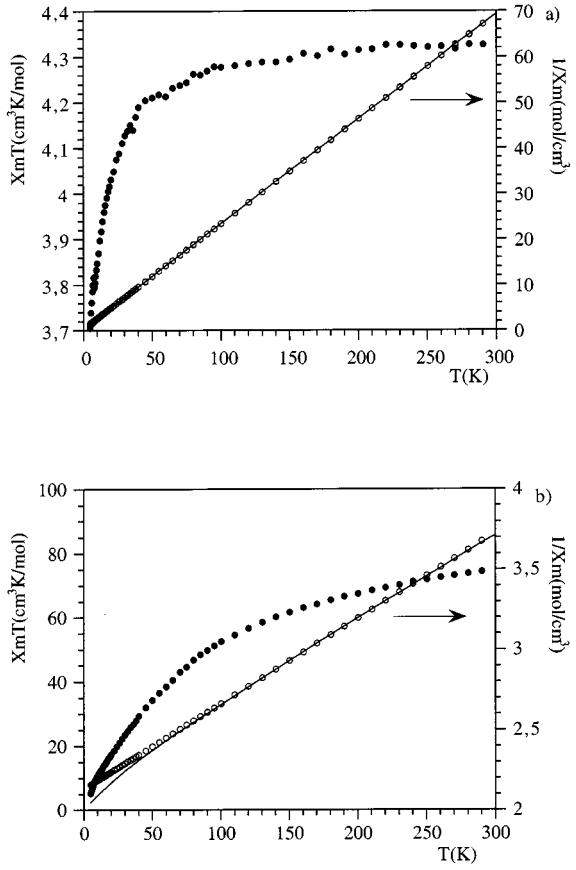

Figure 4. Thermal variations of the magnetic susceptibility ($\chi_m{}^{-1}$) and ($\chi_m T$) for $[SrM(C_3H_2O_4)_2(H_2O)_5] \cdot 2\,H_2O$ compounds a) M = Mn, b) M = Co

Thermal treatments in air and under nitrogen were performed for all compounds. The TG curves are shown in Figure 5. The decomposition steps can be explained as three consecutive processes: namely dehydration, ligand pyrolysis, and evolution of the inorganic residue. The dehydration process occurs in the 70−190°C range, and it is in good accordance with the loss of the seven water molecules present in the complexes. This process seems to take place in only one step, except for the SrNi compound. However, this fact does not allow the presence of different water molecules to be deduced, as was previously observed from the structural data. After a period of stability, ligand pyrolysis occurs at around 350°C. As can be expected, and considering the nature of the cations coordinated to the malonate

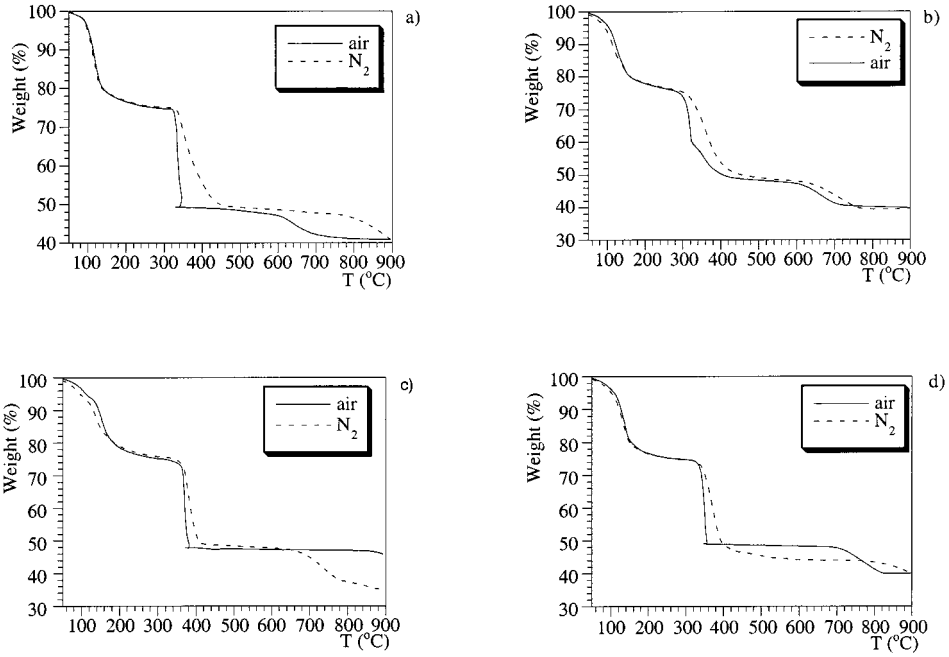

Figure 5. TGA curves for the $[SrM(C_3H_2O_4)_2(H_2O)_5] \cdot 2\,H_2O$ compounds, a) M = Mn, b) M = Fe, c) M = Ni, d) M = Co, in air (−) and under nitrogen (- - -)

ligand,[20] the weight loss is in good accordance with the formation of the products obtained from its decarboxylation, such as the corresponding transition metal oxide and $SrCO_3$. This fact can be attributed to the very high stability of the alkaline-earth metal carbonates. This step remains stable until temperatures above 650°C, when carbonates undergo decomposition to yield mixed oxides. In fact, it is in this process where some differences have been observed between the treatments in air and under nitrogen. The formation of mixed oxides is obviously favoured in air. In this way, the $SrMnO_{3-x}$, $SrCoO_{2.52}$, and $SrFeO_{3-x}$ oxides have been identified by X-ray diffraction as pure phases.[21] However, in the case of the nickel compound, the final residue is formed by the mixture of NiO and $SrCO_3$. The decomposition processes under nitrogen gave rise to a mixture of phases (carbonates, metal oxides, mixed oxides) in all compounds.

In order to improve the above results and to obtain more information about the mixed oxides, thermal treatments in tubular furnaces were performed in air and under nitrogen. In this case, the malonate precursors were fired at 400°C for 12 h. to remove the organic part, followed by treatments at higher temperatures. The resulting products were characterised by IR, X-ray powder diffraction (Figure 6) and differential thermal analysis (DTA).

The metallic ions exhibit mixed valence state in all compounds obtained. In order to propose a chemical formula for all the oxides the oxidation states for the different cations have been determined by a titration method. The samples were dissolved under nitrogen in a solution of HCl, which reacts with metals in the formal +3 and +4 oxidation state. The evolving gas is collected in a solution of KI and after that, titrated with thiosulfate.[22]

The thermal decomposition of the manganese organometallic precursor at 650°C for 10 h gave rise to the non-stoichiometric $SrMnO_{3-x}$ oxide.[23] This product exhibits a dark brown color. The results of the titration analysis are consistent with the formula $SrMnO_{2.95}$. The X-ray diffraction pattern of this phase has been indexed on the basis of an orthorhombic cell with parameters a = 9.437(3), b = 5.453(2) and c = 9.083(4) Å (Figure 6). It is important to note the difference observed between this oxide and that reported in the literature which was obtained from the ceramic method. This latter compound is stoichiometric and crystallises in the hexagonal system. The presence of mixed valence Mn^{3+}/Mn^{4+}, together with a distortion to an orthorhombic symmetry, appears at temperatures above 1035°C. This fact can be due to the creation of oxygen vacancies in the compound.[24] The cell parameters of this non-stoichiometric oxide are similar to those given for $SrMnO_{2.95}$ which was obtained by using the organometallic method. Taking into account these results, and with the aim of confirming the presence of a mixed valence in the last phase, we performed further IR and ESR experiments. The IR spectrum shows two broad bands at around 600 cm^{-1} and 400cm^{-1} (Figure 7a), which could be assigned to the ν_3 stretching vibration corresponding to the $Mn^{3+}-O$ and $Mn^{4+}-O$ bonds, respectively, as usually appears in perovskites with mixed valences.[25] The split of the bands is indicative of a lowering in the symmetry of the manganese environment, probably due to the presence of oxygen vacancies in the surrounding of these ions.

The ESR spectra of this oxide at different temperatures are given in Figure 8a. As can be observed, an isotropic signal appears at room temp. with an ΔHpp value of 960 G. The intensity of the signal decreases with decreasing

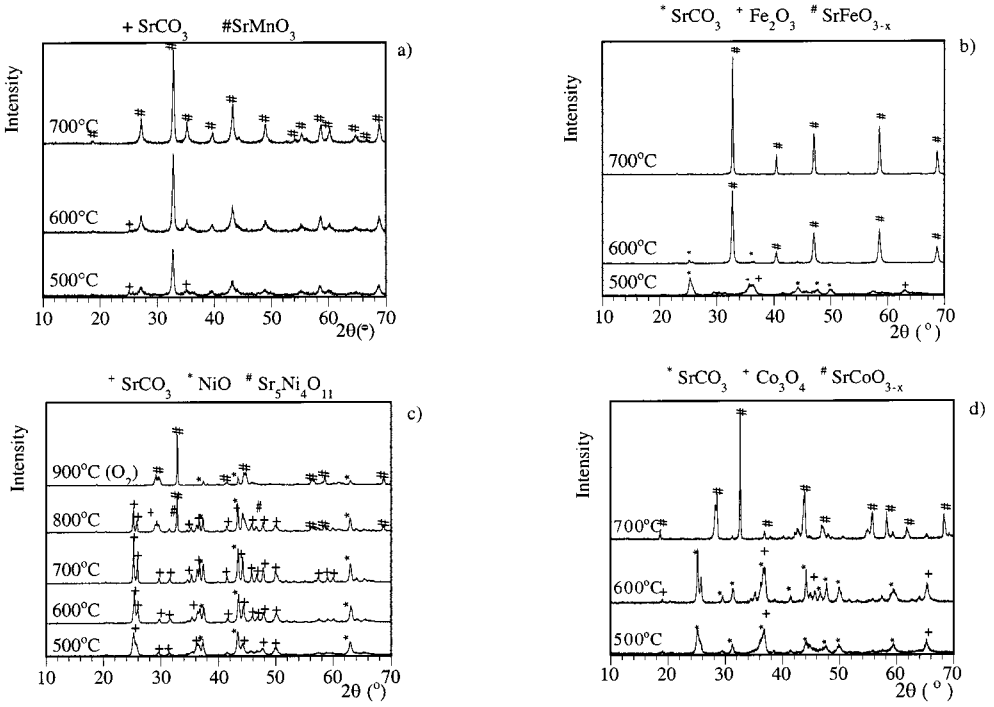

Figure 6. X-ray diffraction patterns of the phases obtained at different temperatures from the $[SrM(C_3H_2O_4)_2(H_2O)_5] \cdot 2\,H_2O$ precursors, a) M = Mn, b) M = Fe, c) M = Ni, d) M = Co

temp., being undetectable at temperatures less than 250 K. These results are characteristic of compounds with antiferromagnetic interactions. Taking into account that the ESR spectra of Mn^{4+} ions show a very broad signal, the results obtained for this phase can be explained as due to the presence of a small amount of Mn^{3+} ions in the compound. These results are in good agreement with those obtained from chemical analyses.

From the decomposition of the $[SrFe(C_3H_2O_4)_2(H_2O)_5] \cdot 2\,H_2O$ phase, the $SrFeO_{2.86}$ oxide[26] was obtained at 650°C for 10 h. The oxygen content was deduced from titration. The X-ray diffraction pattern (Figure 6) has been indexed on the basis of a tetragonal unit cell, *P*4*mm*, with parameters $a = 3.853(4)$ and $c = 3.861(2)$ Å. In order to observe the presence of non-stoichiometry in this phase, ATD measurements under argon were carried out up to 1100°C. An endothermic peak was observed at around 620°C, which would correspond to the reduction of the phase giving rise to the $SrFeO_{2.5}$ stoichiometric oxide. When cooling this sample to room temp. an ordered brown millerite-like structure is obtained. This ordered phase undergoes a reversible transition to the disordered cubic structure at 840°C. These results are in good agreement with those given in the literature for this phase.[27] In order to study the presence of a mixed valence state for the transition metal, IR spectra and ESR measurements in the $SrFeO_{2.86}$ oxide were carried out. As can be seen in the IR spectrum (Figure 7b), no absorption band was observed in the range 600−400 cm^{-1}, as would be expected for a perovskite with mixed valence Fe^{3+}/Fe^{4+}. This result can be explained on the basis of a short range hopping between the Fe^{3+}/Fe^{4+} positions.[27] The ESR spectrum shows an isotropic signal with a *g* value of 2.006 (Figure 8b). This result, together with the value of 620 G for the linewidth, confirms the presence of mixed valence Fe^{3+}/Fe^{4+} in this phase.

The decomposition of the $[SrNi(C_3H_2O_4)_2(H_2O)_5] \cdot 2\,H_2O$ precursor at low temperatures (500−700°C) yielded a mixture of $SrCO_3$ and NiO. The $Sr_5Ni_4O_{11}$ mixed oxide was obtained only after thermal treatments up to 800°C;[28] however, the presence of NiO appears as an impurity phase in the final product (Figure 6). Further attempts to oxidise the total amount of Ni^{II} were unsuccessful.

Thermal treatments of the $[SrCo(C_3H_2O_4)_2(H_2O)_5] \cdot 2\,H_2O$ compound at 700°C for 10 h., gave rise to the formation of the $SrCoO_{2.56}$ phase. Several days at 1100°C were necessary to obtain the mixed oxide from the ceramic method.[29] The X-ray diffraction pattern of the $SrCoO_{2.56}$ phase shows the presence of peaks related to the 2H-Perovskite-type structure. However, not all the diffraction peaks were indexed with this kind of structure. The diffraction patterns do not undergo any significant changes when the compounds are obtained from different thermal treatments under both oxygen and nitrogen. The chemical analysis indicates the presence of a small amount of Co^{IV} in the sample. In order to corroborate this result, further spectroscopic and magnetic measurements were carried out. The IR spectrum shows the characteristic bands at 600 and 400 cm^{-1} (see Figure 7c), corresponding to the ν_3 stretching vibration of $Co^{3+}-O$ and $Co^{4+}-O$ bonds, respectively. Magnetic measurements on this $SrCoO_{2.56}$ oxide were carried out in the temperature range of 1.8−300 K. The thermal evolution of the $\chi_m T$ and χ_m^{-1} is shown in Figure 9.

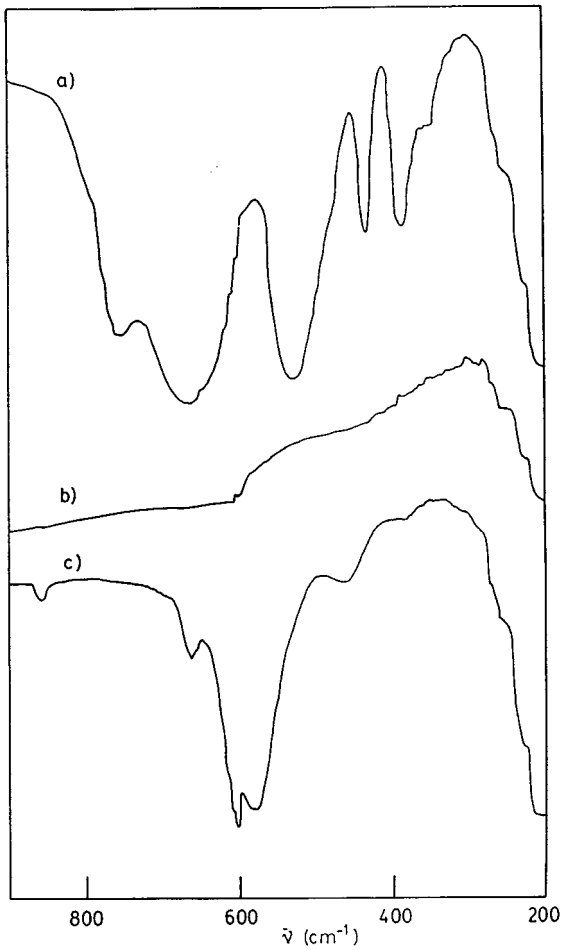

Figure 7. IR spectra of the a) $SrMnO_{2.95}$ b) $SrFeO_{2.86}$, and c) $SrCoO_{2.55}$ oxides

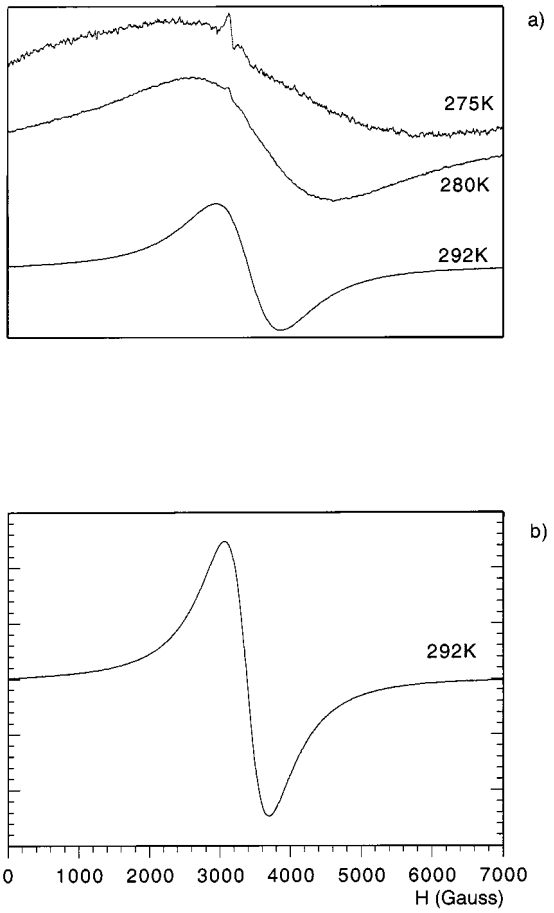

Figure 8. X-band ESR spectra for the a) $SrMnO_{2.95}$ and b) $SrFeO_{2.86}$ phases

The continual decrease observed in the $\chi_m T$ vs T curve is indicative of the presence of an antiferromagnetic ordering, with a Neel temperature value at around 25 K. It is to note an increase of the $\chi_m{}^{-1}$ values at low temperatures, which can be explained as due to the presence of a small amount of Co^{IV}, hampering the total compensation of the Co^{III} spin moments.

A scanning electron microscopic photograph of one of the oxide pellets is shown in Figure 10. In all cases, powders consisting of small homogeneous particles were observed, due to the use of soft synthesis methods. The $SrFeO_{2.86}$ oxide was obtained at the lowest temp., 650°C, and particles with a very small size (diameter less than 0.3 μm) have been favoured.

The more the temperature increases, the higher the size of the grains. Furthermore, particles with a prismatic form have been observed for the $SrCoO_{2.55}$ compound.

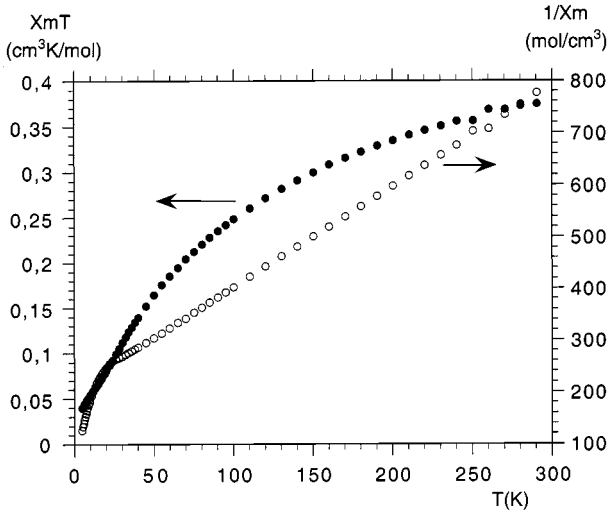

Figure 9. Thermal variation of the χ^{-1} and $\chi_m T$ product for the $SrCoO_{2.55}$ compound

Conclusions

With the aim of obtaining $SrMO_{3-x}$ oxides using soft synthesis routes, four isostructural complexes with the formula $[SrM(C_3H_2O_4)_2(H_2O)_7]$ (M = Mn, Fe, Co, Ni) have been synthesised and characterised. The structure of $[SrCo(C_3H_2O_4)_2(H_2O)_5] \cdot 2\,H_2O$ consists of a 3D network of metal ions coordinated by malonate ligand bridges. The cobalt(II) centres adopt an octahedral coordination while the strontium ions are surrounded by nine oxygen atoms. Magnetic measurements indicate the presence of weak anti-

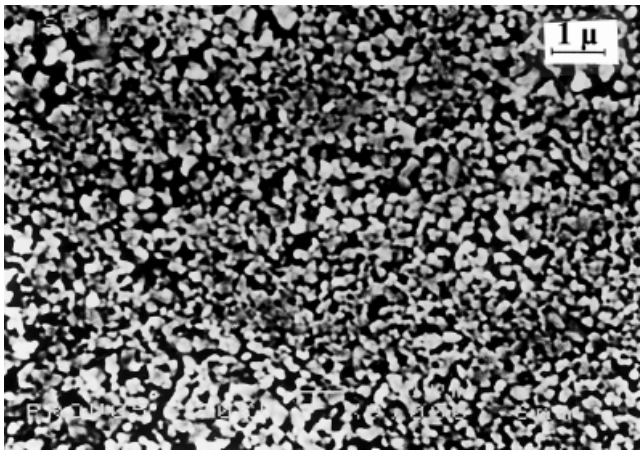

Figure 10. SEM photograph of the $SrMnO_{2.95}$ oxide

ferromagnetic interactions in all compounds. For the cobalt compound, the effect of a spin-orbit coupling must also be considered when discussing the magnetic behaviour. The decomposition steps of the metallo-organic phases, as well as the temperatures in which the evolution of the inorganic residue occurs, were deduced from the TGA studies. This information was utilised in order to perform the thermal treatments, in tubular furnaces, with the aim of obtaining mixed oxides. Depending on the reaction conditions (temperature, reaction time, atmosphere employed, etc.) control of the stoichiometry of these mixed oxides has been achieved. In this way, the oxides with stoichiometry $SrFeO_{2.86}$, $SrCoO_{2.56}$, and $SrMnO_{2.95}$ were synthesised at 600, 700, and 650°C, respectively. The appearance of Co^{IV} in $SrCoO_{2.56}$ and the presence of Mn^{III} in the $SrMnO_{2.95}$ phase is of note. This last oxide was obtained as a stoichiometric phase when synthesised using ceramic methods. The use of soft synthesis methods have also afforded homogeneous and small size particles of oxides, which have been visualised by scanning electron microscopy. In conclusion, it has been shown that from a metallo-organic precursor non-stoichiometric mixed oxides have been obtained at much lower temperatures and reaction times than those employed using the ceramic method

Experimental Section

General: IR: Mattson FTIR 1000 spectrophotometer between 400−4000 cm^{-1}, KBr disks. − Diffuse reflectance spectra: Cary 2415 spectrometer in the range 5000−45000 cm^{-1}, room temp. − Thermogravimetric measurements: Perkin−Elmer System-7 DSC-TGA, crucibles containing 20 mg of sample were heated at 5°/min under dry nitrogen and in air. − DTA: Setaran atd 92 equipment under argon. − Powder X-ray diffraction: Philips X-PERT diffractometer with Cu-$K_{\alpha 1}$ radiation, data were collected by scanning in the range 5° < 2θ < 120° with increments of 0.02°(2θ). − Magnetic susceptibilities and field dependences of magnetization (up to 7 Tesla): Quantum Design MPMS-7 Squid magnetometer, temperature range 1.8−300 K. − ESR: Bruker ESP300 spectrometer, equipped with a standard Oxford low-temperature device operating at X and Q bands, magnetic field was measured with a Bruker bnm 200 gaussmeter, and the frequency was determined with a Hewlett−Packard 5352B microwave frequency counter. Nickel(II) chloride, iron(II) chloride, sodium carbonate, and malonic acid were purchased from Aldrich Co. Strontium chloride was purchased from Merck and cobalt(II) and manganese(II) chlorides from Fluka. All of them were used without further purification.

Preparation of the Compounds: The corresponding chloride of the transition metal (3.0 mmol) was added to an aq. solution of 6.0 mmol (0.624 g) of malonic acid, neutralized with sodium carbonate. The reaction mixture was stirred without heating for about 1 h, and then an equimolar amount of strontium chloride added. The addition of ethanol (3 mL) afforded polycrystalline powders of all phases. In the case of the iron compound a closed system with nitrogen was employed. For the cobalt compound, pale pink crystals in the form of needles were collected after leaving the remaining solution for some days. The compounds were washed with water and acetone, and dried over P_2O_5. The crystals were of good quality for X-ray single-crystal studies. Attempts to obtain single crystals for the other compounds have been unsuccessful. Elemental analysis, together with Inductively Coupled Plasma measurements, were carried out in order to determine the C, H, and metal contents. − $C_6H_{18}MnO_{15}Sr$ (472.75): calcd. C 15.24, H 3.84, Mn 11.62, Sr 18.54; found C 14.94, H 3.21, Mn 11.51, Sr 17.91. − $C_6H_{18}FeO_{15}Sr$ (473.65): calcd. C 15.22, H 3.83, Fe 11.79, Sr 18.50; found C 14.93, H 3.52, Fe 11.52, Sr 19.00. − $C_6H_{18}CoO_{15}Sr$ (476.75): calcd. C 15.12, H 3.81, Co 12.36, Sr 18.38; found C 15.34, H 3.49, Co 12.11, Sr 18.47. − $C_6H_{18}NiO_{15}Sr$ (476.51): calcd. C 15.12, H 3.81, Ni 12.32, Sr 18.39; found C 15.40, H 3.59, Ni 12.86, Sr 17.62.

X-ray Crystal.Structural Determination of $[SrCo(C_3H_2O_4)_2(H_2O)_7]$: Pale pink crystals of $C_6H_{18}SrCoO_{15}$ were sealed in a glass capillary and used for data collection. Preliminary cell dimensions were calculated by Weissenberg photographs. Diffraction experiments were performed with a crystal of dimensions 0.6 × 0.1 × 0.05 mm using an Enraf-Nonius CAD4 automatic diffractometer with graphite-monochromatized Mo-K_α radiation (λ = 0.7107 Å) and the ω-scan technique. Orientation matrix and lattice parameters were determined by least-squares refinement of the diffraction data from 25 machine-centred high-angle reflections in the range 10° < 2θ < 26°. Intensities and angular positions of two standard reflections were measured every 2 h, and these showed neither decrease nor misalignment during data collection. The observed systematic extinctions were consistent with the space group $P2_1/c$. Lorentz and polarization corrections and an empirical absorption correction using XABS2 program were applied to the data.[30] The structure was solved by Patterson interpretation using the program Shelxs86.[31] It was then refined by full-matrix methods based on F^2, using Shelx93.[32] Non-hydrogen atomic scattering factors were taken from International Tables for X-ray Crystallography[33] and anisotropic thermal parameters were assigned. Difference Fourier synthesis did not allow the location of H atoms. Therefore, the hydrogen atoms of the malonate groups were calculated and isotropic thermal parameters were assigned. The final difference Fourier map showed no peaks higher than 0.70 or lower than −0.83 e $Å^{-3}$. The geometric calculations were performed with Parst[34] and Bondla[35] and molecular illustration were drawn with Platon94[36] and Atoms.[37] Crystallographic data (excluding structure factors) for the structure reported in this paper have been deposited with the Cambridge Crystallographic Data Centre as supplementary publication no. CCDC-106908. Copies of the data can be obtained free of charge on application to CCDC, 12 Union Road, Cambridge CB2 1EZ, UK [Fax: int. code + 44-1223/336-033; E-mail: deposit@ccdc.cam.ac.uk].

Acknowledgments

This work has been carried out with the financial support of the Ministerio de Educación y Ciencia (DGICYT PB94−0469 Grant) which we gratefully acknowledge. I. G. M. thanks the Spanish Government for a Doctoral Fellowship.

[1] A. Fujimori, *J. Phys. Chem. Solids* **1992**, *53*, 1595.
[2] [2a] M. Abbate, F. M. F. de Groot, J. C. Fuggle, A. Fujimori, O. Strebel, F. Lopez, M. Domke, G. Kaindl, G. A. Sawatzky, M. Takano, Y. Takeda, H. Eisaki, S. Uchida, *Phys. Rev. B* **1992-II**, 4511. − [2b] T. Arima, Y. Tokura, J. B. Torrance, *Phys. Rev. B: Condens. Matter* **1993-I**, *48*, 17006.
[3] K. Kumagai, T. Suzuki, Y. Taguchi, Y. Okada, Y. Fujishima, Y. Tokura, *Phys. Rev. B* **1993-II**, *48*, 7636.
[4] S. Nakamura, S. Iida, *Jpn. J. Appl. Phys.* **1995**, *34,* L291.
[5] T. Negas, R. S. Roth, *J. Solid State Chem.* **1970**, *1*, 409.
[6] K. J. Lee, E. Iguchi, *J. Solid State Chem*. **1995**, *114*, 242.
[7] [7a] D. W. Meadowcraft, *Nature* **1970**, *226*, 847. − [7b] M. R. Tarasevich, B. F. Efremev, in *Electrodes of Conductive Metallic Oxides* (Ed.: S. Trasatti), Elsevier, New York, **1980**, p. 221.
[8] K. C. Patil, *Bull. Mater. Sci.* **1993**, *16*, 533.
[9] B. N. Sivasankar, S. Govindarajan, *Mater. Res. Bull.* **1996**, *31*, 47.
[10] [10a] M. Insausti, R. Cortés, M. I. Arriortua, T. Rojo, E. H. Bocanegra, *Solid States Ionics* **1993**, *63−65*, 351. − [10b] M. Insausti, J. L. Pizarro, L. Lezama, R. Cortés, E. H. Bocanegra, M. I. Arriortua, T. Rojo, *Chem. Mater.* **1994**, *6*, 707. − [10c] J. García-Jaca, J. I. R. Larramendi, M. Insausti, M. I. Arriortua, T. Rojo, *J. Mater. Chem.* **1995**, *5*, 1995.
[11] [11a] N. J. Ray, B. J. Hathaway, *Acta Crystallogr*. **1982**, *B38*, 770. − [11b] D. Chattopadhyay, S. K. Chattopadhyay, P. R. Lowe, C. H. Schwalbe, S. K. Mazumder, A. Rana, S. Ghosh, *J. Chem Soc., Dalton Trans.* **1993**, 913.
[12] S. M. Saadeh, L. T. Kathleen, J. W. Kampf, W. E. Hatfield, V. L. Pecoraro, *Inorg. Chem*. **1993**, *32*, 3034.
[13] I. Gil de Muro, F. A. Mautner, M. Insausti, L. Lezama, M. I. Arriortua, T. Rojo, *Inorg. Chem*. **1998**, *37,* 3243.
[14] D. Chattopadhyay, S. K. Chattopadhyay, P. R. Lowe, C. H. Schwalbe, S. K. Mazumder, A. Rana, S. Ghosh, *J. Chem. Soc., Dalton Trans.* **1993**, 913.
[15] E. L. Muetterties, L. Guggenberger, *J. Am. Chem. Soc.* **1974**, *96*, 1748.
[16] FULLPROF, J. Rodriguez-Carvajal, *Physica, B* **1992**, *192*, 55.
[17] K. Nakamoto, *Infrared Spectra of Inorganic and Coordination Compounds*, 4th ed., John Wiley & Sons, New York, **1986**.
[18] A. B. P. Lever, *Inorganic Electronic Spectroscopy*, Elsevier Science, Amsterdan, **1984**.
[19] T. M. Dunn, *Trans. Faraday Soc*. **1961**, *57*, 1441.
[20] M. Insausti, I. Gil de Muro, L. Lorente, T. Rojo, E. H. Bocanegra, M. I. Arriortua, *Thermochim. Acta* **1996**, *287*, 81.
[21] *Powder Diffraction File*, Cards Nos. 25-900, 40-1018, 33-678, Joint Committe on Powder Diffraction Standards, Swarthmore, PA, **1984**.
[22] B. E. Gushee, L. Katz, R. Ward, *J. Am. Chem. Soc.* **1957**, *79*, 5601
[23] *Powder Diffraction File*, Card No. 25-900, Joint Committe on Powder Diffraction Standards, Swarthmore, PA, **1984**.
[24] [24a] T. Negas, R. S. Roth, *J. Solid State Chem.* **1970**, *1*, 409. − [24b] P. D. Battle, T. C. Gibb, C. W. Jones, *J. Solid State Chem.* **1988**, *74*, 60. − [24c] K. J. Lee, E. Iguchi, *J. Solid State Chem*. **1995**, *114*, 242.
[25] [25a] R. P. S. M. Lobo, F. Grevais, *Solid State Commun.* **1996**, *98*, 61. − [25b] M. A. Subramanian, *J. Solid State Chem*. **1994**, 111, 134.
[26] *Powder Diffraction File*, Card No. 33-678, Joint Committe on Powder Diffraction Standards, Swarthmore, PA, **1984**.
[27] L. Fournès, Y. Patin, G. Grenier, G. Demazeau, M. Pouchard, *Solid State Commun.* **1987**, *62*, 239.
[28] J. Lee, G. F. Holland, *J. Solid State Chem.* **1991**, *93*, 267.
[29] J. C. Grenier, L. Fournès, M. Pouchard, P. Hagenmuller, *Mat. Res. Bull*. **1986**, *21*, 441.
[30] S. Parkin, B. Moezzi, H. Hope *J. Appl. Crystallogr.* **1995**, *28*, 53.
[31] G. M. Sheldrick *Acta Crystallogr*. **1990**, *A46*, 467.
[32] G. M. Sheldrick, *SHELX93, Program for the Refinement of Crystal Structures*, University of Göttingen, Germany, **1993**.
[33] *International Tables for X-ray Crystallography*, vol. IV, Kynoch Press, Birmingham, U. K., **1974**, p. 72−98.
[34] M. Nardelli. PARST, *Comp. Chem.* **1983**, *7*, 95−98.
[35] J. M. Stewat (Ed.), *The X-ray System, Technical Report TR-446 of the Computer Science Center*, University of Maryland, College Park, Maryland, **1976**.
[36] A. L. Spek, *PLATON94, Program for the Automated Analysis of Molecular Geometry*, **1994**.
[37] E. Dowty, *ATOMS, A Computer Program for Displaying Atomic Structures*, version 2.0, Kingsport, TN, **1993**.

Received November 9, 1998
[I98388]